THERMODYNAMIC EQUILIBRIUM DISTRIBUTION OF PARTICLES IN 2-D ELECTRIC FIELD

by

Yuanxing Zhang

A thesis submitted to Johns Hopkins University in conformity with the requirements for the degree of Master of Science

Baltimore, Maryland

May 2019

Abstract

We study the particles in the colloidal system under a two-dimensional electric field: the way to assemble the particles in the Brownian dynamic simulation and the equilibrium density profile of the system derived by considering the particle-field interaction and the equation of state for hard colloidal particles.

In the research, the software COMSOL Multiphysics is used to solve the anisotropic electric field in a lookup table form to work the same as an analytical expression of the field property, which is not available. And triangular interpolation is used to make the lookup table work for every position in the plane.

We develop the way to solve the equilibrium density profile given any electric field conditions in the 2D plane and work that on three types of electric field, then simulation is performed to verify our theory.

Advisor: Michael A. Bevan

Reader: Joelle Frechette

Acknowledgements

Thanks to Bevan Lab,

especially my advisor Dr. Bevan and my senior labmate Jianli Zhang!

Table of Contents

List of Figures

Chapter 1 Introduction

1.1 Particle behavior under external field

The influence of an external field on the colloidal particles under it is very common in nature and in research. In natural and living systems, equilibrium and out-of-equilibrium assemblies are good examples, such as the navigation of some Magnetotactic bacteria (MTB)[1], bacterial colonies' synchronized fluorescent blinking[2] and some camouflage mechanisms[3]. Colloidal particles sediment under the gravitational field[4-5], which is quite common in the lab and daily life. In research, multiple ways have been developed to assemble particles, like particles assemble into long chains in high-frequency electric fields between coplanar electrodes[6], the magnetic field is also used in research to remove superparamagnetic particles in the aqueous dispersion[7], and light-absorbing particles are assembled under thermophoresis by exposed in light.[8] Different kinds of external fields have been applied in areas like nanolithography[9-10], micro-sensors[11] and optical materials[12], as well.

1.2 Colloidal crystal and assembly

Here, the ability to control the position and density of particles without mechanical intervention is what we are concerned. Using electric field is one of the good ways to do this, since it doesn't have much restriction to particle's properties. Unlike other ways mentioned above, common silica particles can assemble in an electric energy landscape generated by multiple electrodes. Optimal methods to assemble spherical colloidal particles into a perfect colloidal crystal has been explored[13-14]. In the past, an isotropic electric field is often used to control the assembly. However, the design and application of the anisotropic one hasn't been reported yet. In this paper, a way to design anisotropic electric field of different potential energy

contour shapes is shown, and it is used in simulating the new assembly policy, which has a better successful rate and a shorter time to take than the former one.

1.3 Particle equilibrium distribution in a colloidal system

In many cases, particles' behavior in these cases are directly relevant to their equilibrium interaction under the field and the thermodynamics of the colloidal system. To have a thorough understanding of particles' behavior and thermodynamic properties under an external field, a theoretical study into it is helpful.

Many phase transition mechanisms and equilibrium phase diagrams with various kinds of colloids[15-17] and states[18-20] have been reported. While recently, the properties of irregular particles with different shapes[21-22] and dynamics[23-25] are widely investigated, as well.

The local particle density profile is of great scientific interest but less understood. The equilibrium density profile of colloidal particles under gravitational field was first reported for simple systems as a model to study molecular systems[4-5, 26-27], then used in the study of the phase transitions in more advanced systems[28-30]. More recently, particle density profile under electric field is also studied[31-34], but the density variates only in one single dimension, thus no previous report that looks into multi-dimensional density profile under electric fields exists yet.

1.4 Work in this paper

Since the equation of state has been used to relate density distribution or phase behavior with energy landscape[35], and the expression of colloidal hard spheres in solid and liquid phase has also been worked out[36-37]. We can figure out a 2-D equilibrium density profile of colloidal particles by solving a series of differential equations. After the equilibrium density distribution is known, we can have a better understanding of phase behavior of the system.

In this work, an optimal method to assemble spherical colloidal particles into a perfect crystal in simulation by alternating two orthogonal anisotropic electric field is developed. Besides, by combining the equation of state of hard particles, energy landscape in the 2-D plane and differential equations of osmotic pressure and particle density, the 2-D equilibrium density profile of colloidal particles under the external field is theoretically worked out. Not only can we verify the simulation with the theoretical calculation result, but the methodology can be applied to other 2-D electric fields.

Chapter 2 Theory

2.1 Particles' interaction in the electric field

For one particle i in the high-frequency AC electric field, the net force on it is given by,

$$F_i = \nabla\left[u_{df,i}^{pf} + \sum_{j\neq i}\left(u_{e,i,j}^{pp} + u_{dd,i,j}^{pp}\right)\right] \tag{1}$$

where $u_{df,i}^{pf}$, $u_{e,i,j}^{pp}$ and $u_{dd,i,j}^{pp}$ represent dipole-field interaction between the particle and the field, electrostatic double layer repulsion between two particles and dipole-dipole interaction between two particles, respectively.

The dipole-field interaction between a particle i located at (x_i, y_i) and the field is given by,

$$u_{df,i}^{pf}(x_i, y_i) = -2\pi\varepsilon_m a^3 f_{cm} E^2(x_i, y_i) \tag{2}$$

where ε_m is the medium dielectric permittivity, a is the diameter of one spherical particle, f_{cm} is the Clausius-Mossotti factor, and E is the local electric field magnitude.

The electrostatic double layer repulsion between particle i and another particle j is given by,

$$u_{e,i,j}^{pp}\left(r_{ij}\right)=32\pi\varepsilon_m a\left(\frac{kT}{e}\right)^2\tanh^2\left(\frac{e\Psi}{4kT}\right)\exp\left[-\kappa\left(r_{ij}-2a\right)\right] \tag{3}$$

where r_{ij} is the distance between the center of particle i and j, κ is the inverse Debye screening length, and ψ is the colloidal surface potential and e is the elemental charge.

The dipole-dipole interaction induced by the electric field between particle i and j is given by,

$$u_{dd,i,j}^{pp}\left(x_i,y_i,\vec{r}_{ij}\right)=-\pi\varepsilon_m a^3 f_{cm}^2 P_2\left(\cos\theta_{ij}\right)\left(\frac{2a}{r_{ij}}\right)^3 E\left(x_i,y_i\right)^2 \tag{4}$$

where $P_2(cos\theta_{ij})$ is the second Legendre polynomial and θ_{ij} is the angle between the line that connects the two particle centers and the local electric field direction.

2.2 Equation of state for the colloidal system

By the equation of state for hard sphere colloids, the expression for the two-dimensional osmotic pressure Π, in terms of the particle number density ρ and the compressibility factor Z, is given as,

$$\Pi(\rho)=kT\rho Z(\rho) \tag{5}$$

Here Z is a function of η, the area fraction,

$$Z_{\mathrm{F}}(\eta)=\left(1+\frac{\eta^2}{8}\right)(1-\eta)^{-2} \qquad \eta<\eta_f$$
$$Z_{\mathrm{S}}(\eta)=2\left(\frac{\eta_{CP}}{\eta_{eff}}-1\right)^{-1}+0.67\left(\frac{\eta_{CP}}{\eta_{eff}}-1\right)+1.9 \quad \eta_m<\eta<\eta_{CP} \tag{6}$$

where Z_F is the compressibility factor for fluid state valid from infinite dilution to the freezing point, $\eta_f = 0.69$; and Z_S is the one for FCC solid state valid from the melting point, $\eta_m = 0.71$, to the close packing, $\eta_{CP} = 0.906$.

The area fraction and the particle number density, is related by,

$$\eta=\pi a^2\rho \tag{7}$$

where a is the radius of the particles in the system.

Eq. (5) can be rewritten by combining Eq. (6) and Eq. (7) as,

$$\Pi(\eta)=kT\frac{\eta}{\pi a^2}\mathrm{Z}(\eta) \tag{8}$$

The model above should be corrected by replacing the actual particle radius a with effective radius a_{eff}, to accommodate the electrostatic repulsion interaction between particles, as,

$$2a_{eff}=2a+\int_{2a}^{\infty}\left[1-\exp\left(-u^{pp}(r)/kT\right)\right]dr \tag{9}$$

Similarly, the particle number density and the area fraction should also be replaced by the effective ones: ρ_{eff} and η_{eff} in all relative theoretical calculation.

2.3 Osmotic pressure differential equation in 2D

In a potential energy landscape, which has its magnitude in 2D, the differential change of the colloid osmotic pressure is given as,

$$\begin{aligned}\frac{\partial \Pi(x,y)}{\partial x} &= -\frac{\partial U(x,y)}{\partial x}\cdot\rho(x,y)\\ \frac{\partial \Pi(x,y)}{\partial y} &= -\frac{\partial U(x,y)}{\partial y}\cdot\rho(x,y)\end{aligned} \tag{10}$$

We rewrite the equations above into the total derivative form to replace them as,

$$d\Pi = -dU\cdot\rho \tag{11}$$

which is applicable to one, two or three dimensions.

2.4 Equilibrium density distribution

We use Eq. (7) and Eq. (8) to substitute for ρ and Π in Eq. (11) and we can get,

$$kT\cdot\eta_{eff}^{-1}d\left[\eta_{eff}\cdot Z\left(\eta_{eff}\right)\right] = -dU \tag{12}$$

Since Z is a piecewise function of η, the integrated form of Eq. (12) is given as,

$$U - U_{ref} = -kT\left\{\int_{\eta_{ref}}^{\eta_m}\frac{1}{\eta_{eff}}d\left(\eta_{eff}\cdot Z_{\mathrm{S}}\right) + \int_{\eta_f}^{\eta}\frac{1}{\eta_{eff}}d\left(\eta_{eff}\cdot Z_{\mathrm{F}}\right)\right\} \tag{13}$$

where η_{ref} and U_{ref} are the effective area fraction and potential energy at the reference state.

Eq. (13) relates effective area fraction and potential energy, and when we insert this relation into the potential energy landscape in 2D, the variation of potential energy is replaced by the variation of effective area fraction, so that the density distribution in equilibrium is achieved. Meanwhile, the following relation should hold,

$$N = \int_{-\infty}^{+\infty}\int_{-\infty}^{+\infty} \rho(x,y)\,dxdy \tag{14}$$

where N is the number of particles in the system, and it is related to the reference state used in solving for Eq. (13).

2.5 Crystalline Order Parameters in 2D

The six-fold bond orientational order parameter is given by,

$$\psi_6^i = \frac{1}{N^i}\sum_{j=1}^{N^i} e^{i6\theta_{ij}} \tag{15}$$

where N^i is 'coordination number', defined as number of neighbor particles that are within the first coordination radium of particle i.

Thus, we have the crystalline connectivity,

$$\chi_6^{ij} = \frac{\left|\mathrm{Re}\left[\psi_6^i \psi_6^{j*}\right]\right|}{\left|\psi_6^i \psi_6^{j*}\right|} \tag{16}$$

where ψ_6^{j*} is the complex conjugate of ψ_6^j.

Then the local and global average six-fold connectivity order parameter, C_6^i and C_6, which are defined as the number of crystalline neighbors near each particle in an ensemble and the average density of the ensemble, respectively, can be given as,

$$C_6^i = \frac{1}{6}\sum_{j=1}^{N^i}\left[\begin{vmatrix} 1 & \chi_6^{ij} \geq 0.32 \\ 0 & \chi_6^{ij} < 0.32 \end{vmatrix}\right] \tag{17}$$

and,

$$C_6 = \frac{1}{N}\sum_{i=1}^{N} C_6^i \tag{18}$$

Chapter 3 Method

3.1 COMSOL Multiphysics

The medium and electrode properties were established in COMSOL Multiphysics. A model chamber was setup, which had a volume of 400 μm by 400 μm by 40 μm and filled with 0.1mM NaOH water solution as the medium. Each of the gold octupole electrode cylinders was 20 μm in diameter and 40nm in thickness, whose top/bottom centers were on the vertices of a regular octagon with 100 μm diagonal distance. **Fig. 1** shows the top view of the chamber in the software's geometry part, while the material of each part and the electric potential of each electrode should be set according to our design. In our paper, three types of electric fields are designed, which will be shown in the result part.

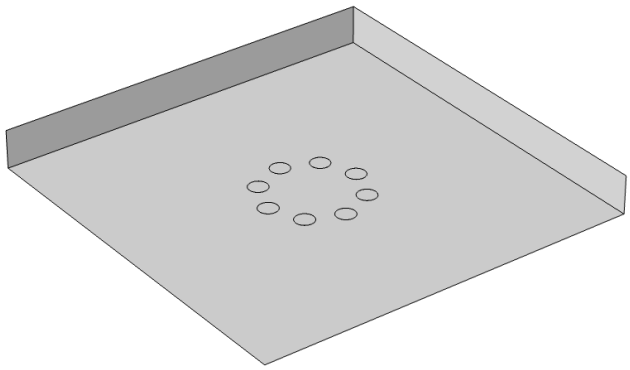

Fig. 1 The geometry interface in COMSOL Multiphysics software, in the figure the three-dimensional model of the electrode design is shown.

Then the electric field was solved numerically, and a lookup table was obtained at the height of 1.5 μm from the bottom surface, which is the height of the particle center, with a resolution of 0.25 μm by 0.25 μm. The lookup table contained the electric field properties needed in the simulation code and potential energy landscape calculation with Eq. (2). **Fig. 2** shows the properties contained in the lookup table and the lookup table option.

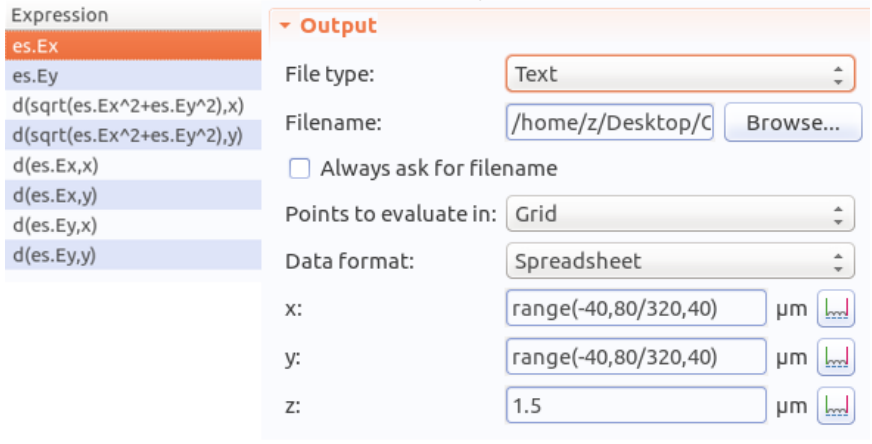

Fig. 2 The electric parameters expression contained in the lookup table and the output option.

3.2 Triangular interpolation

Since we get a look up table with parameters at coordinates in a fixed interval, now we must find a way to get the field properties of points that are not on the lookup table.

Here we use the triangular interpolation, since the interval of the lookup table is much smaller than the particle size, the average assumption could be trusted. First we find out the nearest three points on the lookup table grid to the point k we are studying, and calculate the distance from them r_1, r_2, r_3, if the property Q on the table is to be studied and shows to be Q_1, Q_2, Q_3 on the point, respectively. Then we have,

$$Q_k = \frac{\frac{Q_1}{r_1} + \frac{Q_2}{r_2} + \frac{Q_3}{r_3}}{\frac{1}{r_1} + \frac{1}{r_2} + \frac{1}{r_3}} \tag{19}$$

3.3 Brownian dynamic simulation

Brownian dynamic simulation was used in assembling particles into a colloidal crystal. Also, the equilibrium distribution of a fixed number of particles in the electric field was obtained through this method. The particles are all 3 μm in diameter and the force balance of each of them was given by Eq. (1), where the electric field was solved with triangular interpolation based on particle coordinate and the lookup table obtained by COMSOL Multiphysics.

For each case of electric condition and particle number, at least 3000 cycles of simulation were performed to get the equilibrium distribution. The particles equilibrated from a random starting distribution in each cycle. The resolution of the density profile is 1 μm by 1 μm.

Chapter 4 Result

4.1 Anisotropic Electric Fields and Potential Energy Landscape

Three types of electric field contour shapes are shown in **Fig. 3**(A-C), and the electric potential energy landscapes under corresponding conditions, are shown in **Fig. 3**(D-F). The electrodes are shown as the surrounding circles, and applied voltages on them are represented by the filled grayscale colors. These voltages are normalized by V_{pp}, which is defined as the voltage applied to west-east pairs and is fixed at 3V in all cases. The electric field contours are normalized using E_0, which is defined as $E_0 = \frac{V_{pp}}{dg}$. And the energy landscapes are drawn in the unit of thermo energy kT with respect to the corresponding potential energy calculated using Eq.

(2). The electric fields and energy landscapes are plotted up to $2E_0$ and $30kT$, respectively, to distinguish the different spatial variation patterns.

The different shapes of normalized fields and energy landscapes shown in **Fig. 3** are determined by the ratio of the voltages applied to the west-east and north-south electrodes. To be specific, by applying equal voltages to the two pairs of electrodes, the generated electric field and energy landscape are isotropic (**Fig. 3A&D**); While if different voltages are applied to the two pairs of electrodes, the fields and energy landscapes become anisotropic (**Fig. 3B&C, E&F**). These fields are identified by their voltage ratios, respectively V_{pp}: V_{pp}, V_{pp}: $0.6V_{pp}$, and

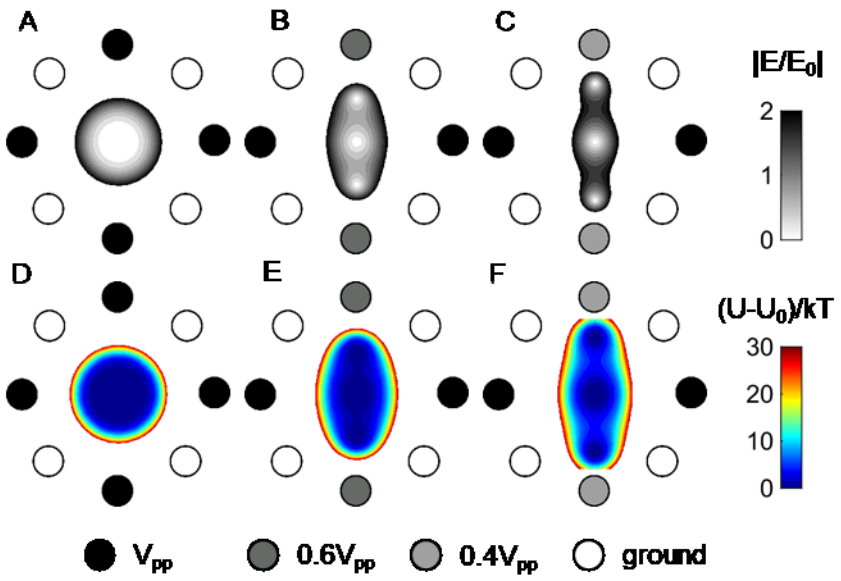

Fig. 3 (A-C) Electric field magnitudes plotted using grayscale contours. The electrode voltages are normalized by the reference voltage of $V_{pp} = 3.0V$, which is defined as the voltage applied to west-each electrodes, and the field magnitudes are normalized by $E_0 = \frac{V_{pp}}{dg}$ and plotted near the field center. In order to achieve the above field shapes, the voltage ratios applied to the west-east and north-south electrodes are set to be (A) 1:1, (B) 1:0.6, and (C) 1:0.4. (D-F) Corresponding potential energy landscapes defined with respect to the center of the field. The landscapes are also plotted near the field center and show the most significant differences in the contour shapes.

V_{pp}: $0.4V_{pp}$, and these energy landscapes will be used to study the equilibrium distribution of

particles.

4.2 The Brownian dynamic simulation using lookup table

In **Fig. 4**, several frames from the Brownian dynamic simulation are shown. We take the case that a total number of 300 particles assemble in an isotropic electric field generated by applying a voltage ratio of V_{pp}: V_{pp} as an example. The reference voltage V_{pp} is set as 3.0V. The particles are scattering in the middle of the electrodes evenly using the random engine mt19937

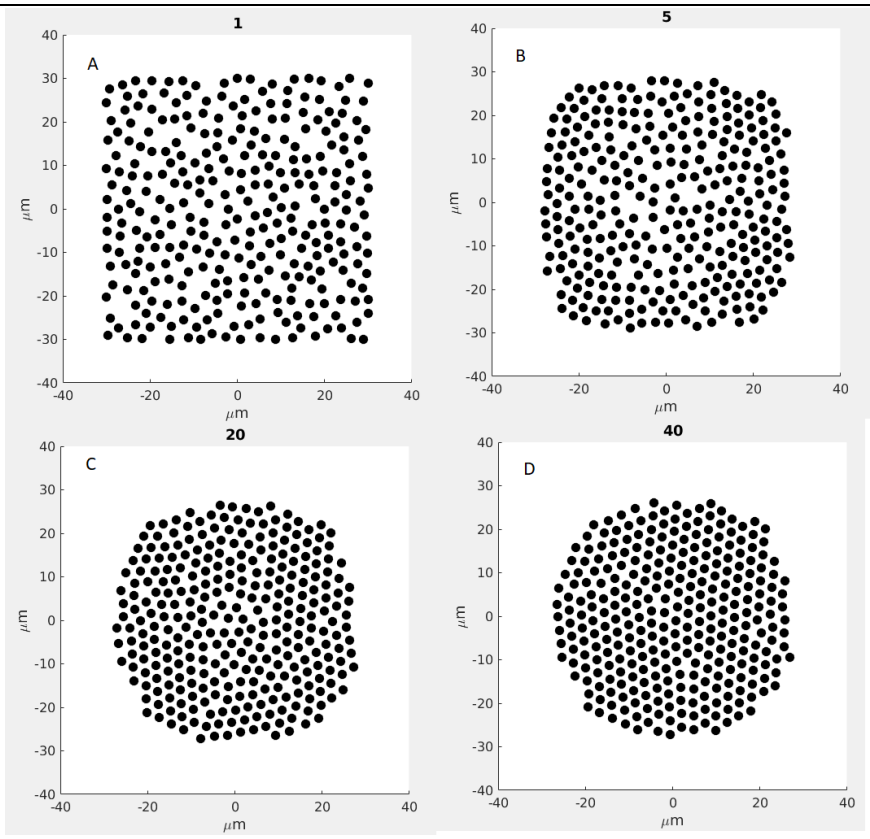

Fig.4 Snapshots taken from the Brownian dynamic simulation of 300 silica particles under the electric field generated by applying a voltage ratio of V_{pp}: V_{pp} as an example. The reference voltage V_{pp} is set as 3.0V. (A-D) Snapshots taken at time 0s, 5s, 20s, 40s, which represent the starting random distribution (A), the early stage of the simulation (B), the starting formation of the colloidal crystal (C) and the colloidal crystal fully influenced by the electric field, or the equilibrium distribution (D), respectively.

(**Fig. 4A**), then we turn on the voltage and they assemble quickly affected under the effect of the electric field (**Fig. 4B**), and at about 20s, a colloidal crystal in solid state, which is yet not so condensed, starts to form (**Fig. 4C**), and at 40s, as the system is under the influence of the electric field for time long enough, a steady colloidal crystal is formed, and the electric field can hardly change the structure of this crystal (**Fig. 4D**). If we are unsatisfied with the structure obtained, we can only change to another electric field or turn off the electric field to release the particles to the fluid state.

4.3 Equilibrium Distribution in the theory and simulation

Theoretical equilibrium distributions of a total number of 100 particles under the electric field achieved by applying different voltage ratios, calculated based on Eq. (13) is shown in **Fig. 5.** In **Fig. 5A, D, G**, a votage ratio of V_{pp}: V_{pp} is applied to form the isotropic distribution, while

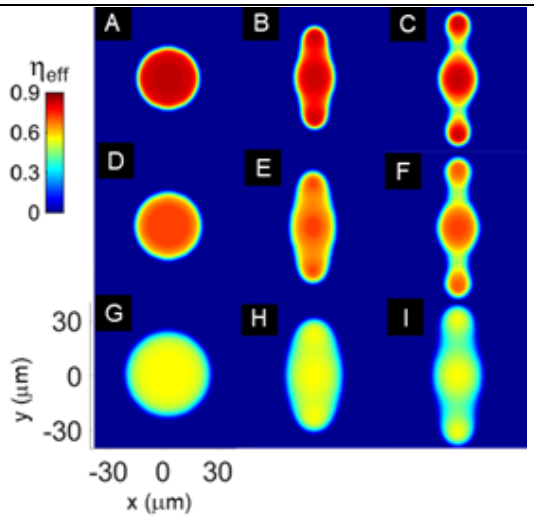

Fig. 5 Theoretical equilibrium distributions of a total number of 100 particles under the electric field achieved by applying different voltage ratios, calculated based on Eq. (13). The reference area fractions η_{ref} are fixed as 0.83 (A-C), 0.73 (D-F), and 0.55 (G-I) to represent the solid, transitional, and fluid phase respectively. While the distribution shape is determined by the voltage ratio appied, as V_{pp}: V_{pp}(A, D, G), V_{pp}: $0.6V_{pp}$(B, E, H), V_{pp}: $0.4V_{pp}$(C, F, I). The required reference voltages V_{pp} are found to be 3.8V (A), 3.3V (B), 2.5V (C), 2.2V (D), 1.9V (E), 1.6V (F), 0.9V (G), 0.9V (H), 0.8V (I), respectively.

in comparation, the anisotropic distributions formed from the votage ratio of V_{pp}: $0.6V_{pp}$ and V_{pp}: $0.4V_{pp}$ are also shown in **Fig. 5B, E, H** and **Fig. 5C, F, I**.

The particle number and preset reference area fractions are fixed to solve for the required voltage conditions for each case. The energy-density relationship with same targeted reference area fraction is same for different field shapes, because Eq. (13) illlustrates that the relationship is independent of the field properties like magnitude and spatial variation. On the other side, because of the lack of analytical solution to the field, or the energy landscape, the problem was solved recursively as followed: starting from an initial field condition, the voltage ratio and the reference voltage, the energy landscape is substituted for a distribution of effective area fraction

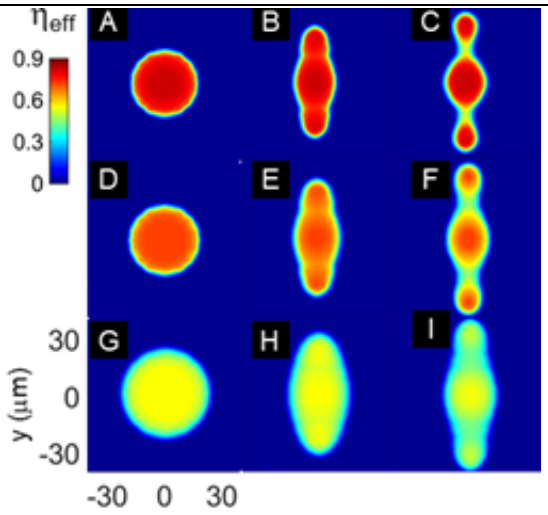

Fig. 6 Statistic measurement of equilibrium distributions of a total number of 100 particles under the electric field achieved by applying different voltage ratios, obtained by performing Brownian dynamic simulation. The reference area fractions η_{ref} are fixed as 0.83 (A-C), 0.73 (D-F), and 0.55 (G-I) to represent the solid, transitional, and fluid phase respectively. While the distribution shape is determined by the voltage ratio appied, as V_{pp}: V_{pp}(A, D, G), V_{pp}: $0.6V_{pp}$(B, E, H), V_{pp}: $0.4V_{pp}$(C, F, I). The required reference voltages V_{pp} are found to be 3.8V (A), 3.3V (B), 2.5V (C), 2.2V (D), 1.9V (E), 1.6V (F), 0.9V (G), 0.9V (H), 0.8V (I), respectively.

using the energy-density relationship. Next the total number of particle within the distribution is

calculated using Eq. (14), which is then compared with the targeted particle number, and the field condition is changed accordingly. And the reference voltages are found to be 3.8V (A), 3.3V (B), 2.5V (C), 2.2V (D), 1.9V (E), 1.6V (F), 0.9V (G), 0.9V (H), 0.8V (I), respectively.

Statistic measurement of equilibrium distributions of a total number of 100 particles under the electric field achieved by applying different voltage ratios, obtained by performing Brownian dynamic simulation is shown in **Fig. 6**. All the conditions are set the same as the theory part and the way to do draw the distribution figure has been illustrated in the method part.

In order to compare the result from the theory and the simulation, one-dimensional distribution profiles in positive y-axis is given in **Fig. 7**. For different reference area fraction, theoretical estimations are shown using solid line (0.83), dash line (0.73), and dot line (0.55), and the simulation results are shown using square, circle, and triangle marks respectively. The plots and the lines fit very well in all cases.

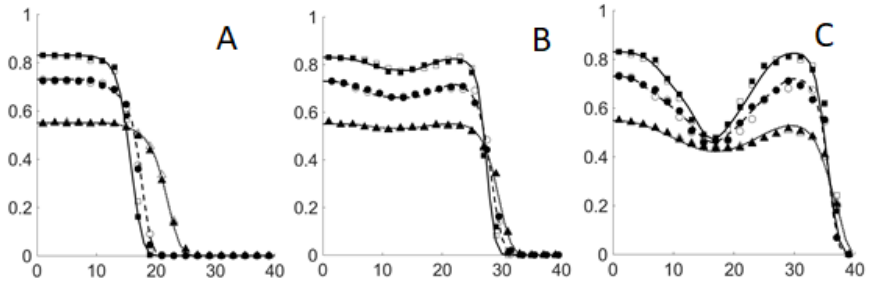

Fig. 7 One-dimensional distribution profiles in positive y-axis. The reference area fractions are taken the same as those in **Fig. 4&5**. For different reference area fraction, theoretical estimations are shown using solid line (0.83), dash line (0.73), and dot line (0.55), and the simulation results are shown using square, circle, and triangle marks respectively. The open marks are obtained using the simulation with field-induced dipolar interaction considered, and closed marks are obtained without this interaction in the simulation.

Chapter 5 Conclusion and future work

In this essay, we report the study of equilibrium distribution of colloidal particles under the 2D electric field. Anisotropic field is an important method and tool in solving the topic, a series of which is generated using an octupole electode. To overcome the difficulty to get an analycal expression of the anisotropic field, COMSOL Multiphysics is used to solve for the field and output one lookup table for one field, which is used in calculating the potential energy landscape for the theory derivation and also for the simulation of particles in an electric field. The theoretical equilibrium distribution is derived by combining the particle-field interaction and the equation of state for hard spheres in the colloidal system.

With the result in this essay, the conditions needed for an equilibrium state can be easily calculated, giving the number of particles in the system. This could be used not only to determine the electrode design for assembling particles into a crystal with perticular shape, but also to adjusting the voltage to make the local density at any position in one electric field to be the value we want, thus we are able to control the phase behavior in the system, even in the lab experiment, this would be useful.

Reference

1. Faivre, D.; Schüler, D., Magnetotactic Bacteria and Magnetosomes. *Chemical Reviews* **2008,** *108* (11), 4875-4898.
2. Din, M. O.; Danino, T.; Prindle, A.; Skalak, M.; Selimkhanov, J.; Allen, K.; Julio, E.; Atolia, E.; Tsimring, L. S.; Bhatia, S. N.; Hasty, J., Synchronized cycles of bacterial lysis for in vivo delivery. *Nature* **2016,** *536*, 81.
3. Teyssier, J.; Saenko, S. V.; van der Marel, D.; Milinkovitch, M. C., Photonic crystals cause active colour change in chameleons. *Nature Communications* **2015,** *6*, 6368.
4. Beckham, R. E.; Bevan, M. A., Interfacial colloidal sedimentation equilibrium. I. Intensity based confocal microscopy. *The Journal of Chemical Physics* **2007,** *127* (16), 164708.
5. Lu, M.; Bevan, M. A.; Ford, D. M., Interfacial colloidal sedimentation equilibrium. II. Closure-based density functional theory. *The Journal of Chemical Physics* **2007,** *127* (16), 164709.
6. Fraden, S.; Hurd, A. J.; Meyer, R. B., Electric-field-induced association of colloidal particles. *Physical Review Letters* **1989,** *63* (21), 2373-2376.
7. Ge, J.; Hu, Y.; Biasini, M.; Beyermann, W. P.; Yin, Y., Superparamagnetic Magnetite Colloidal Nanocrystal Clusters. *Angewandte Chemie International Edition* **2007,** *46* (23), 4342-4345.
8. Schmidt, F.; Liebchen, B.; Lowen, H.; Volpe, G., Light-controlled assembly of active colloidal molecules. *J Chem Phys* **2019,** *150* (9), 094905.
9. Zhang, G.; Wang, D.; Möhwald, H., Ordered Binary Arrays of Au Nanoparticles Derived from Colloidal Lithography. *Nano Letters* **2007,** *7* (1), 127-132.
10. Deckman, H. W.; Dunsmuir, J. H., Natural lithography. *Applied Physics Letters* **1982,** *41* (4), 377-379.
11. Cai, Z.; Smith, N. L.; Zhang, J. T.; Asher, S. A., Two-dimensional photonic crystal chemical and biomolecular sensors. *Anal Chem* **2015,** *87* (10), 5013-25.
12. Nasilowski, M.; Mahler, B.; Lhuillier, E.; Ithurria, S.; Dubertret, B., Two-Dimensional Colloidal Nanocrystals. *Chemical Reviews* **2016,** *116* (18), 10934-10982.
13. Tang, X.; Rupp, B.; Yang, Y.; Edwards, T. D.; Grover, M. A.; Bevan, M. A., Optimal Feedback Controlled Assembly of Perfect Crystals. *ACS Nano* **2016,** *10* (7), 6791-6798.
14. Edwards, T. D.; Beltran-Villegas, D. J.; Bevan, M. A., Size dependent thermodynamics and kinetics in electric field mediated colloidal crystal assembly. *Soft Matter* **2013,** *9* (38), 9208-9218.
15. Anderson, V. J.; Lekkerkerker, H. N. W., Insights into phase transition kinetics from colloid science. *Nature* **2002,** *416* (6883), 811-815.
16. Troppenz, T.; Filion, L.; van Roij, R.; Dijkstra, M., Phase behaviour of polarizable colloidal hard rods in an external electric field: a simulation study. *The Journal of chemical physics* **2014,** *141* (15), 154903.
17. Zaccarelli, E., Colloidal gels: equilibrium and non-equilibrium routes. *Journal of Physics: Condensed Matter* **2007,** *19* (32), 323101.
18. Palberg, T., *Crystallization kinetics of colloidal model suspensions: Recent achievements and new perspectives*. 2014; Vol. 26.
19. Karthika, S.; Radhakrishnan, T. K.; Kalaichelvi, P., A Review of Classical and Nonclassical Nucleation Theories. *Crystal Growth & Design* **2016,** *16* (11), 6663-6681.
20. Li, B.; Zhou, D.; Han, Y., Assembly and phase transitions of colloidal crystals. *Nature Reviews Materials* **2016,** *1*, 15011.
21. Kalyuzhnyi, Y. V.; Jamnik, A.; Cummings, P. T., Melting upon cooling and freezing upon heating: fluid–solid phase diagram for Švejk–Hašek model of dimerizing hard spheres. *Soft Matter* **2017,** *13* (6), 1156-1160.

22. Kuijk, A.; Troppenz, T.; Filion, L.; Imhof, A.; van Roij, R.; Dijkstra, M.; van Blaaderen, A., Effect of external electric fields on the phase behavior of colloidal silica rods. *Soft Matter* **2014,** *10* (33), 6249-6255.
23. Palacci, J.; Cottin-Bizonne, C.; Ybert, C.; Bocquet, L., Sedimentation and Effective Temperature of Active Colloidal Suspensions. *Physical Review Letters* **2010,** *105* (8), 088304.
24. Rezvantalab, H.; Beltran-Villegas, D. J.; Larson, R. G., Rotator-to-Lamellar Phase Transition in Janus Colloids Driven by Pressure Anisotropy. *Physical Review Letters* **2016,** *117* (12), 128001.
25. Du, C. X.; van Anders, G.; Newman, R. S.; Glotzer, S. C., Shape-driven solid-solid transitions in colloids. *Proceedings of the National Academy of Sciences of the United States of America* **2017,** *114* (20), E3892-E3899.
26. Rutgers, M. A.; Dunsmuir, J. H.; Xue, J. Z.; Russel, W. B.; Chaikin, P. M., Measurement of the hard-sphere equation of state using screened charged polystyrene colloids. *Physical Review B* **1996,** *53* (9), 5043-5046.
27. Löwen, H., Colloidal soft matter under external control. *Journal of Physics: Condensed Matter* **2001,** *13* (24), R415-R432.
28. Ginot, F.; Theurkauff, I.; Levis, D.; Ybert, C.; Bocquet, L.; Berthier, L.; Cottin-Bizonne, C., Nonequilibrium Equation of State in Suspensions of Active Colloids. *Physical Review X* **2015,** *5* (1), 011004.
29. Pusey, P. N.; van Megen, W., Phase behaviour of concentrated suspensions of nearly hard colloidal spheres. *Nature* **1986,** *320* (6060), 340-342.
30. Luigjes, B.; Thies-Weesie, D. M. E.; Philipse, A. P.; Erné, B. H., Sedimentation equilibria of ferrofluids: I. Analytical centrifugation in ultrathin glass capillaries. *Journal of Physics: Condensed Matter* **2012,** *24* (24), 245103.
31. Yethiraj, A.; Wouterse, A.; Groh, B.; van Blaaderen, A., Nature of an Electric-Field-Induced Colloidal Martensitic Transition. *Physical Review Letters* **2004,** *92* (5), 058301.
32. Sullivan, M. T.; Zhao, K.; Hollingsworth, A. D.; Austin, R. H.; Russel, W. B.; Chaikin, P. M., An Electric Bottle for Colloids. *Physical Review Letters* **2006,** *96* (1), 015703.
33. Zhang, K.-Q.; Liu, X. Y., In situ observation of colloidal monolayer nucleation driven by an alternating electric field. *Nature* **2004,** *429* (6993), 739-743.
34. Juárez, J. J.; Feicht, S. E.; Bevan, M. A., Electric field mediated assembly of three dimensional equilibrium colloidal crystals. *Soft Matter* **2012,** *8* (1), 94-103.
35. Percus, J. K., Equilibrium state of a classical fluid of hard rods in an external field. *Journal of Statistical Physics* **1976,** *15* (6), 505-511.
36. Alder, B. J.; Hoover, W. G.; Young, D. A., Studies in Molecular Dynamics. V. High‐Density Equation of State and Entropy for Hard Disks and Spheres. *The Journal of Chemical Physics* **1968,** *49* (8), 3688-3696.
37. Henderson, D., Monte carlo and perturbation theory studies of the equation of state of the two-dimensional Lennard-Jones fluid. *Molecular Physics* **1977,** *34* (2), 301-315.

VITA

Name: Yuanxing Zhang

Address: Yuanxing Zhang may be contacted through Dr. M. A. Bevan
at the Chemical and Biomelecular Engineering Department,
Johns Hopkins University,
Baltimore, MD 21218

Email: yzhan318@jhu.edu

Education: B.S., Material Science and Engineering, Tsinghua University, 2013, China